Geometric Attitude Control of a Small Satellite for Ground Tracking Maneuvers

Barry B. Goeree and Brian Shucker
Advisor — Dr. Ernest D. Fasse

Aerospace and Mechanical Engineering Dept.
University of Arizona, Tucson, AZ 85721
{goeree, bshucker}@u.arizona.edu

Abstract. The UASat is a small satellite being designed by students from the University of Arizona. The UASat is being designed to be launched from the Hitchhiker Ejection System. One of its scientific missions is to receive laser communication signals from a ground station. In order to receive the signals, the telescope of the satellite must track the ground station while passing over. This paper describes the kinematics and control of this ground tracking maneuver. The parameters of the nonlinear control law have a geometrical, intuitive interpretation which simplifies their selection. Simulation results are shown for the maneuver.

1 Introduction

This paper describes the attitude control laws of the UASat. This section introduces the UASat project and gives an overview of the mission, orbit, attitude control system (ACS) and control modes. After this context is given, the paper will focus on attitude control of the ground tracking maneuver.

1.1 The UASat Project

The Student Satellite Project is the cooperative effort of students at the University of Arizona to design and build UASat[9]. The UASat has several scientific and technical missions. The primary science objective is the detection and imaging of lightning and sprites. Sprites are high-altitude lightning-like phenomena. The secondary science objective is photometering of stars. The technical mission is to receive laser communication signals from a ground station. These experiments are to be carried out with a single integrated optical system.

The UASat is being designed to be launched from the Hitchhiker Ejection System (HES). The Hitchhiker Ejection System poses constraints on the physical dimensions of the satellite which are summarized in Tab. 1. The orbital parameters used to design UASat are given in Tab. 2.

Figure 1 shows the 8-sided structure of the UASat. The telescope is mounted along the center line of the satellite. Solar panels are mounted on all 8 sides.

Table 1: Hitchhiker Ejection System constraints on physical dimensions of the satellite

Max. weight	68 Kg (150 lb)
Max. height	52 cm (20.5 in)
Max. diameter	50 cm (20 in)
Max. distance c.g. from canister centerline	1.27 cm (0.5 in)
Max. distance c.g. from separation plane	26 cm (10.25 in)

Table 2: Orbital parameters

Inclination	ι	51.6°
Altitude		407 km
Right ascending node	Ω	TBD
Argument of perigee	ω	0
Eccentricity	e	0
Orbit period		92.7 minutes

Power is limited to 25-30W continuous due to the limited surface area for solar panels. Deployable solar arrays are not an option as they would increase drag and shorten the mission lifetime drastically.

1.2 The Attitude Control System (ACS)

There are three control modes to support the science and technical missions. In addition to these mission specific modes there are two modes to perform other tasks like detumbling and orienting the satellite with respect to the Sun to maximize power generation.

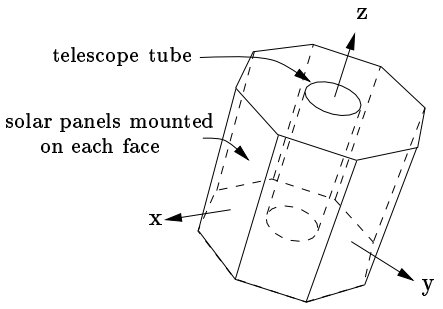

Figure 1: The UASat employs a single telescope mounted along the centerline. Solar panels are mounted on all eight faces.

The control modes can be summarized as follows.

Limb pointing: The primary science objective is the imaging of lightning and sprites. Sprites can only be observed when the telescope is pointing at the limb of the earth. The satellite must maintain a fixed attitude with respect to the earth, keeping the telescope pointing at the horizon.

Inertial pointing: The secondary science objective is photometering of stars. The attitude of the satellite must be stabilized with respect to the stars so that the telescope points at a particular star.

Ground tracking: The technical mission is to receive laser communication signals from a ground station. In order to receive signals, the satellite must track the ground station while passing over. From a controls point of view this is the most demanding experiment as it requires a high degree of accuracy at relatively high maneuver rates.

Maximum power generation: Power is very limited on the UASat due to the limited surface area for solar panels. Therefore if the satellite is on the sun side, the solar cells have to be perpendicular to the incoming rays of sunlight so that power generation is maximized. To minimize thermal gradients the satellite must also spin around the telescope axis.

Safe mode: The satellite must be able to detect an emergency situation and recover if possible. This mode is a collection of several tasks including detumbling of the satellite. Details of this mode will not be given in this paper.

The specifications for each control mode are given in Tab. 3. Not all specifications are determined at this time. The specifications are driven by the design of the science instrument and will be adjusted when the design evolves. The current set of specifications is used to design the control algorithms.

Table 3: ACS specifications for each mode

Mode	Accuracy	Jitter	Ref.
Limb pointing	2° R,P; 0.4° Y	TBD	Earth
Inertial pointing	1°	TBD	stars
Ground tracking	1°	TBD	Earth
Max. power gen.	10°	TBD	Sun

The control modes require a combination of inertial and Earth based pointing. To support all modes the UASat will employ 3-axis control. Four reaction wheels are used for redundancy. In addition to the reaction wheels, three magneto-torquers are used to dump momentum. A GPS, a magnetometer, coarse sunsensors and a horizon sensor are used to obtain information about the satellite's attitude. The sensor information is processed by a Kalman filter that estimates the attitude and angular velocity of the satellite. The design of the attitude estimation system is an important and critical task but outside the scope of this paper. Assume for the rest of the paper that an accurate attitude estimate is available.

From an attitude control point of view, the ground tracking mode is the most challenging. The rest of this paper will focus on the kinematics and control of this maneuver.

1.3 Relation to Prior Work

Traditional attitude control is based on linear control theory[15]. The nonlinear rotational dynamics are linearized around selected design states. Linear control is simple and design methods are well established. However, linear control is only valid for small attitude error and nonintuitive for large attitude errors. Meyer[10] was one of the first to apply nonlinear control to the attitude control problem. He used Lyapunov control theory to find control laws that are globally stable. His excellent technical report[10] motivated and inspired later papers in geometric control theory[1, 8]. Other approaches to nonlinear attitude control are sliding mode control[3, 12], linearizing transformations[2] and nonlinear optimal control[14]. The control law presented in this paper is a nonlinear geometric controller.

The attitude of a satellite can be represented in many different ways[13]. Often attitude error mea-

sures are defined as the algebraic differences between actual and desired attitude parameters[3, 12]. Although attitude parameters themselves may be geometric, their algebraic difference is generally not. For example, Euler parameters are geometric entities but the difference of two Euler parameters is not in general an Euler parameter. This difference can be used as an index of error, but it is not a Euclidean geometric entity. Few researchers represent the attitude error as a rotation between the actual and desired attitude[10, 11]. The controller presented in this paper uses the relative rotation between the desired and actual attitude as a Euclidean geometric measure of attitude error.

The contribution of this paper is the application of a geometrical control law to ground tracking maneuvers. The nonlinear control law provides stability for large attitude errors as long as the reaction wheel torques do not saturate. The control parameters have a geometrical, intuitive interpretation for small attitude errors which simplifies their selection. Linear design techniques can actually be used to determine those parameters.

The rest of this paper is organized as follows. Section 2 introduces the notation and defines the reference frames that are used in this paper. Section 3 describes the kinematics of the ground station tracking maneuver. The control law is explained in Sec. 4. Simulation results are given in section 5. Finally, the paper will be concluded in section 6.

2 Notation and Coordinate Frames

Vectors will be denoted by lowercase boldface letters. Matrices will be denoted by uppercase boldface letters. Scalars are denoted by italic lowercase letters. For example the eigenvalue problem is written as $\mathbf{Ax} = \lambda\mathbf{x}$. In general, let $\tilde{\mathbf{a}}$ denote the *cross-product matrix* of vector $\mathbf{a}$, the 3×3 skew-symmetric matrix such that $\tilde{\mathbf{a}}\mathbf{b} = \mathbf{a} \times \mathbf{b}$ for any vector $\mathbf{b}$. Algebraically, $\tilde{\mathbf{a}}$ is given by

$$\tilde{\mathbf{a}} = \begin{bmatrix} 0 & -a_3 & a_2 \\ a_3 & 0 & -a_1 \\ -a_2 & a_1 & 0 \end{bmatrix} \tag{1}$$

The coordinate frame of reference is denoted by a superscript. For example, the vector $\mathbf{x}^{\text{eci}}$ is given in coordinates of the ECI-frame. The following reference frames are used throughout the paper.

Spacecraft Frame (SCF) The origin of the spacecraft-fixed SCF frame is at the center of mass of the satellite. The z-axis points along the bore sight of the telescope axis. The x-axis is perpendicular to the z-axis and points to the center of the first side panel. The y-axis is chosen such that a right-handed orthonormal reference frame is formed. The SCF-frame is shown in Fig. 1.

Desired Frame (D) The origin of the desired frame is at the center of mass of the satellite. The axes of the frame form an orthonormal triplet and represent the desired attitude of the satellite. The attitude error is zero if the spacecraft frame and the desired frame are aligned.

Earth-Centered Inertial Frame (ECI) The ECI frame is centered at the Earth and is fixed with respect to the stars. The z-axis points at the celestial pole. The x-axis points toward the mean equinox, the direction from the Earth to the sun on the first day of spring. The y-axis is chosen such that a right-handed orthonormal triplet is formed. The ECI-frame is shown in Panel (a) of Fig. 2.

Earth-Fixed Frame (ECF) The ECF frame is fixed with respect to the Earth. Its origin is at the center of the earth. The z-axis points at the celestial pole. The x axis runs through the prime meridian. The y-axis is chosen such that a right-handed orthonormal reference frame is formed. The ECF-frame is shown in Panel (a) of Fig. 2.

Orbit Frame (ORB) The origin of the orbit frame is at the center of the Earth. The z-axis correspond to the orbit normal, and the x-axis is in the direction from the Earth centroid to the ascending node. The y-axis follows from the right hand rule. The orbit-frame is shown in Panel (b) of Fig. 2.

The attitude of a rigid body may be defined by a reference frame attached to the rigid body[13]. The spacecraft-fixed frame will be used to define the attitude of the satellite with respect to the ECI-frame. Denote the frame vectors of the spacecraft-fixed frame in ECI coordinates with $\mathbf{e}^{\text{eci}}_{1,\text{sc}}, \mathbf{e}^{\text{eci}}_{2,\text{sc}}$ and $\mathbf{e}^{\text{eci}}_{3,\text{sc}}$. Then the direction cosine matrix

$$\mathbf{A}^{\text{eci}}_{\text{sc}} = \begin{bmatrix} \mathbf{e}^{\text{eci}}_{1,\text{sc}} & \mathbf{e}^{\text{eci}}_{2,\text{sc}} & \mathbf{e}^{\text{eci}}_{3,\text{sc}} \end{bmatrix} \tag{2}$$

will be interpreted as the spacecraft attitude with respect to inertial space. Similarly, the desired attitude is represented with a desired frame $\mathbf{A}^{\text{eci}}_{\text{d}} = \begin{bmatrix} \mathbf{e}^{\text{eci}}_{1,\text{d}} & \mathbf{e}^{\text{eci}}_{2,\text{d}} & \mathbf{e}^{\text{eci}}_{3,\text{d}} \end{bmatrix}$ where $\mathbf{e}^{\text{eci}}_{1,\text{d}}, \mathbf{e}^{\text{eci}}_{2,\text{d}}$ and $\mathbf{e}^{\text{eci}}_{3,\text{d}}$ are

the frame vectors of the desired frame in ECI-coordinates.

3 Ground Station Tracking

The technical mission is to receive laser communication signals from the ground. In order to receive these signals, the telescope must be pointing at the ground station while passing over. This motion specifies a desired attitude, angular velocity and acceleration which the controller tracks. The controller is described in Sec. 4. In this section the kinematic equations for the desired motion will be derived.

3.1 Desired Attitude

First expressions for the locations of the ground station and the the satellite will be derived. These expressions are subtracted from each other and the result normalized to get a unit vector in the direction from the satellite to the ground station. This unit vector is used to specify a desired attitude $\mathbf{A}_{\mathrm{d}}^{\mathrm{eci}}$.

The location of the ground station is given by

$$\mathbf{x}_{\mathrm{G}}^{\mathrm{eci}} = \mathbf{A}_{\mathrm{ecf}}^{\mathrm{eci}} \mathbf{x}_{\mathrm{G}}^{\mathrm{ecf}} \tag{3}$$

where $\mathbf{A}_{\mathrm{ecf}}^{\mathrm{eci}}$ is the transformation matrix from ECF to ECI coordinates. Let λ_{W} and λ_{N} be the longitude and geocentric latitude of the ground station respectively. Let R_{E} be the distance from the Earth centroid to the the ground station. The coordinates of the ground station are (see Panel (a) of Fig. 2)

$$\mathbf{x}_{\mathrm{G}}^{\mathrm{ecf}} = R_{\mathrm{E}} \begin{bmatrix} \cos\lambda_{\mathrm{N}} \cos\lambda_{\mathrm{W}} \\ \cos\lambda_{\mathrm{N}} \sin\lambda_{\mathrm{W}} \\ \sin\lambda_{\mathrm{N}} \end{bmatrix} \tag{4}$$

Assuming a spherical Earth with the geocentric latitude equal to geodetic latitude[7], the coordinates of the ground station in Tucson are $\lambda_{\mathrm{N}} = 32.19581°$, $\lambda_{\mathrm{W}} = -110.89171°$ and $R_{\mathrm{E}} = 6,378.137\mathrm{km}$.

Assume a circular orbit with radius R_{S} and inclination ι. The orbit is shown in Panel (b) of Fig. 2. For a circular orbit the argument of perigee, ω, is not uniquely defined and can be set to zero: $\omega = 0$. The satellite orbits in the x-y plane of the orbit frame as

$$\mathbf{x}_{\mathrm{S}}^{\mathrm{orb}} = R_{\mathrm{S}} \begin{bmatrix} \cos\nu \\ \sin\nu \\ 0 \end{bmatrix} \tag{5}$$

where ν is the true anomaly. The location of the satellite in ECI coordinates is given by

$$\mathbf{x}_{\mathrm{S}}^{\mathrm{eci}} = \mathbf{A}_{\mathrm{orb}}^{\mathrm{eci}} \mathbf{x}_{\mathrm{S}}^{\mathrm{orb}} \tag{6}$$

where the transformation matrix from orbit to ECI coordinates is

$$\mathbf{A}_{\mathrm{orb}}^{\mathrm{eci}} = \begin{bmatrix} \cos\Omega & -\sin\Omega\cos\iota & \sin\Omega\sin\iota \\ \sin\Omega & \cos\Omega\cos\iota & -\cos\Omega\sin\iota \\ 0 & \sin\iota & \cos\iota \end{bmatrix} \tag{7}$$

where Ω is the angle of right ascension of the orbit.

Let $\mathbf{x}_{\mathrm{G/S}}^{\mathrm{eci}} = \mathbf{x}_{\mathrm{G}}^{\mathrm{eci}} - \mathbf{x}_{\mathrm{S}}^{\mathrm{eci}}$ be the displacement from the satellite to the ground station. The unit vector directed from the satellite to the ground station is

$$\mathbf{u}_{\mathrm{G/S}}^{\mathrm{eci}} = \frac{1}{\|\mathbf{x}_{\mathrm{G/S}}^{\mathrm{eci}}\|} \mathbf{x}_{\mathrm{G/S}}^{\mathrm{eci}} \tag{8}$$

where $\|\mathbf{x}_{\mathrm{G/S}}^{\mathrm{eci}}\|$ is the Euclidean norm of vector $\mathbf{x}_{\mathrm{G/S}}^{\mathrm{eci}}$.

The desired attitude should be such that the telescope points toward the ground station. Therefore, the third column of $\mathbf{A}_{\mathrm{d}}^{\mathrm{eci}}$ is determined by $\mathbf{u}_{\mathrm{G/S}}^{\mathrm{eci}}$. The first two columns are arbitrary as rotations about the telescope axis are not important; $\mathbf{A}_{\mathrm{d}}^{\mathrm{eci}}$ is not completely specified by the problem.

The desired attitude can be determined as follows. Given initial time t_0, let $\mathbf{A}_{\mathrm{d}}^{\mathrm{eci}}(t_0)$ be any orthonormal matrix such that the third column is $\mathbf{u}_{\mathrm{G/S}}^{\mathrm{eci}}(t_0)$. The desired $\mathbf{A}_{\mathrm{d}}^{\mathrm{eci}}(t)$ is determined by integrating the angular velocity:

$$\mathbf{A}_{\mathrm{d}}^{\mathrm{eci}}(t) = \int_{t_0}^{t} \tilde{\boldsymbol{\omega}}_{\mathrm{d}}^{\mathrm{eci}}(\tau) \mathbf{A}_{\mathrm{d}}^{\mathrm{eci}}(\tau) d\tau + \mathbf{A}_{\mathrm{d}}^{\mathrm{eci}}(t_0) \tag{9}$$

This is only necessary because $\mathbf{A}_{\mathrm{d}}^{\mathrm{eci}}(t)$ is not completely specified by the problem. A suitable desired angular velocity $\boldsymbol{\omega}_{\mathrm{d}}^{\mathrm{eci}}$ will be derived in the next section. Once $\mathbf{A}_{\mathrm{d}}^{\mathrm{eci}}(t)$ is known, then the desired angular velocity in spacecraft coordinates can be determined, $\boldsymbol{\omega}_{\mathrm{d}}^{\mathrm{scf}}(t) = [\mathbf{A}_{\mathrm{d}}^{\mathrm{eci}}(t)]^t \boldsymbol{\omega}_{\mathrm{d}}^{\mathrm{eci}}(t)$.

3.2 Desired Angular Velocity

The desired angular velocity is not uniquely specified for this problem. A particular choice with no rotation component about $\mathbf{u}_{\mathrm{G/S}}^{\mathrm{eci}}$ is

$$\boldsymbol{\omega}_{\mathrm{d}}^{\mathrm{eci}} = \tilde{\mathbf{u}}_{\mathrm{G/S}}^{\mathrm{eci}} \dot{\mathbf{u}}_{\mathrm{G/S}}^{\mathrm{eci}} \tag{10}$$

The rate of change of $\mathbf{u}_{\mathrm{G/S}}^{\mathrm{eci}}$ follows by differentiating (8) with respect to time. It can be shown that[5]

$$\dot{\mathbf{u}}_{\mathrm{G/S}}^{\mathrm{eci}} = \frac{1}{\|\mathbf{x}_{\mathrm{G/S}}^{\mathrm{eci}}\|} \left(\mathbf{I}_3 - \mathbf{u}_{\mathrm{G/S}}^{\mathrm{eci}} (\mathbf{u}_{\mathrm{G/S}}^{\mathrm{eci}})^t\right) \dot{\mathbf{x}}_{\mathrm{G/S}}^{\mathrm{eci}} \tag{11}$$

where $\mathbf{I}_3$ is the 3×3 identity matrix. The velocity vector $\dot{\mathbf{x}}_{\mathrm{G/S}}^{\mathrm{eci}}$ can be found by subtracting (6) from (3)

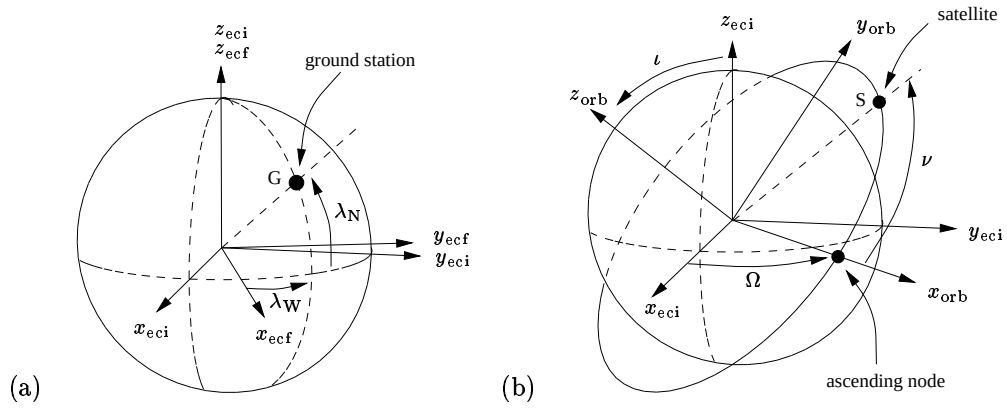

Figure 2: Geometry of ground station on Earth and a circular orbit.

and differentiating the result. Assuming that orbital parameters Ω and ι vary only very slowly in time such that the matrix $\mathbf{A}_{\rm orb}^{\rm eci}$ can be considered constant, it follows that for a fixed ground station

$$\dot{\mathbf{x}}_{\rm G/S}^{\rm eci} = \tilde{\boldsymbol{\omega}}_{\rm sid}^{\rm eci}\mathbf{x}_{\rm G}^{\rm eci} - \mathbf{A}_{\rm orb}^{\rm eci}R_{\rm S}\dot{\nu}\begin{bmatrix}-\sin\nu\\ \cos\nu\\ 0\end{bmatrix} \tag{12}$$

where $\boldsymbol{\omega}_{\rm sid}^{\rm eci} = \begin{bmatrix}0 & 0 & 2\pi/86,164\end{bmatrix}^t$ is the sidereal rotation rate of the Earth and $\dot{\nu}$ is the orbit rate in rad/s. From (10), (11), (12) and using that for any vector $\mathbf{a}$, $\tilde{\mathbf{a}}\mathbf{a} = \mathbf{0}$, it follows that

$$\boldsymbol{\omega}_{\rm d}^{\rm eci} = \frac{1}{\|\mathbf{x}_{\rm G/S}^{\rm eci}\|}\tilde{\mathbf{u}}_{\rm G/S}^{\rm eci}\dot{\mathbf{x}}_{\rm G/S}^{\rm eci} \tag{13}$$

3.3 Desired Angular Acceleration

The desired angular acceleration follows by differentiating (13) with respect to time assuming that $\boldsymbol{\omega}_{\rm sid}^{\rm eci}$, $\mathbf{x}_{\rm G}^{\rm eci}$, $\mathbf{A}_{\rm orb}^{\rm eci}$, $R_{\rm S}$, and $\dot{\nu}$ can be considered constant. Much computation yields

$$\dot{\boldsymbol{\omega}}_{\rm d}^{\rm eci} = \frac{-2}{\|\mathbf{x}_{\rm G/S}^{\rm eci}\|}\boldsymbol{\omega}_{\rm d}^{\rm eci}(\mathbf{u}_{\rm G/S}^{\rm eci})^t\dot{\mathbf{x}}_{\rm G/S}^{\rm eci} + \frac{1}{\|\mathbf{x}_{\rm G/S}^{\rm eci}\|}\tilde{\mathbf{u}}_{\rm G/S}^{\rm eci}\mathbf{A}_{\rm orb}^{\rm eci}R_{\rm S}\dot{\nu}^2\begin{bmatrix}\cos\nu\\ \sin\nu\\ 0\end{bmatrix} \tag{14}$$

4 Control Law

A block diagram of the control law is shown in Fig. 3. The rightmost block represents the attitude dynamics and the state estimation system. Estimates of the actual attitude, $\mathbf{A}_{\rm sc}^{\rm eci}$, actual angular velocity, $\boldsymbol{\omega}_{\rm sc}^{\rm scf}$, of the satellite, and the reaction wheel speeds, $\boldsymbol{\omega}_{\rm rw}$, are the outputs, and the reaction wheel torques, $\boldsymbol{\tau}_{\rm rw}$, are the inputs of this block. The control law computes the reaction wheel torques such that the actual attitude will track the desired attitude.

The control law consists of several terms. The elastic and viscous term are feedback terms. The elastic term implements a spatial spring-like behavior between the desired and actual frame. The torque, $\boldsymbol{\tau}_{\rm el}^{\rm scf}$, acts to align the two frames. The viscous term, $\boldsymbol{\tau}_{\rm visc}^{\rm scf}$, is a damping term that depends on the difference between the actual and desired angular velocity. It provides stability. The model-based compensation is a feed-forward term based on the inverse of the attitude dynamics. The torque, $\boldsymbol{\tau}_{\rm mdl}^{\rm scf}$, would give the satellite the desired angular acceleration if there were no modeling and sensing errors. The sum of the terms describe above is a torque, $\boldsymbol{\tau}_{\rm sc}^{\rm scf}$, acting on the satellite structure. This torque is mapped to reaction wheel torques using the pseudo-inverse of the reaction wheel configuration matrix. Finally, a wheel speed management term, $\boldsymbol{\tau}_{\rm wsm}$, is added to let the reaction wheels operate around a desired speed, $\boldsymbol{\omega}_{\rm rw,d}$. The rest of this section will discuss each term in more detail.

4.1 Elastic Term

The elastic term implements a spatial spring-like behavior that acts to align the actual frame, $\mathbf{A}_{\rm sc}^{\rm eci}$, with the desired frame, $\mathbf{A}_{\rm d}^{\rm eci}$. To derive the elastic term, $\boldsymbol{\tau}_{\rm el}^{\rm scf}$, a potential function is defined. This potential is a function of the relative orientation (attitude error) of the actual and desired frame and corresponds to the energy stored in the spring. The potential function is minimized when the frames are aligned. The torque, $\boldsymbol{\tau}_{\rm el}^{\rm scf}$, can be obtained from the potential

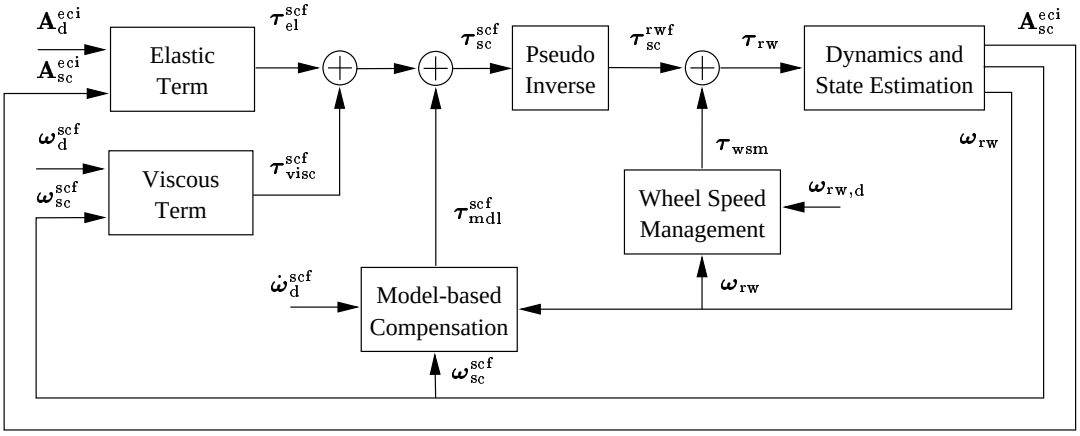

Figure 3: Block diagram of the control law

function using a virtual work argument. We start with introducing the potential function.

Potential function Let $\mathbf{P}$ be a diagonal*, positive-definite matrix of user selectable co-stiffnesses

$$\mathbf{P} = \mathrm{diag}(\pi_1, \pi_2, \pi_3) \tag{15}$$

where $\mathrm{diag}(a, b, c)$ is the diagonal matrix with a, b, c on its diagonal. Define potential function, U, as

$$U = \mathrm{tr}(\mathbf{P}) - \mathrm{tr}(\mathbf{P}(\mathbf{A}_{\mathrm{sc}}^{\mathrm{eci}})^t \mathbf{A}_{\mathrm{d}}^{\mathrm{eci}}) \tag{16}$$

where $\mathrm{tr}(\mathbf{A})$ is the trace of matrix $\mathbf{A}$. Matrix $(\mathbf{A}_{\mathrm{sc}}^{\mathrm{eci}})^t \mathbf{A}_{\mathrm{d}}^{\mathrm{eci}}$ is the relative rotation between the actual and desired frame. The relative rotation matrix is a Euclidean geometric measure of attitude error.

Potential function (16) is a weighted difference of inner products of corresponding frame vectors and is minimized when the frames are aligned. To see this rewrite the second term of (16) as

$$\mathrm{tr}(\mathbf{P}(\mathbf{A}_{\mathrm{sc}}^{\mathrm{eci}})^t \mathbf{A}_{\mathrm{d}}^{\mathrm{eci}}) = \sum_{i=1}^{3} \pi_{\mathrm{i}} (\mathbf{e}_{\mathrm{i,sc}}^{\mathrm{eci}})^t \mathbf{e}_{\mathrm{i,d}}^{\mathrm{eci}} \tag{17}$$

From (16) and (17) follows that the potential function, U, can be written as

$$U = \sum_{i=1}^{3} \pi_{\mathrm{i}} (1 - (\mathbf{e}_{\mathrm{i,sc}}^{\mathrm{eci}})^t \mathbf{e}_{\mathrm{i,d}}^{\mathrm{eci}}) \tag{18}$$

*The co-stiffness matrix $\mathbf{P}$ does not necessarily have to be diagonal. Any symmetric, positive-definite matrix can be used. Any symmetric matrix $\mathbf{P}$ can be expressed in the form $\mathbf{P} = \mathbf{R}\boldsymbol{\Gamma}\mathbf{R}^t$ where $\mathbf{R}$ is orthonormal and $\boldsymbol{\Gamma}$ is a diagonal matrix. The columns of the orthonormal matrix $\mathbf{R}$ determine the principal stiffness axes. In this paper $\mathbf{R}$ is chosen to be the identity matrix. The principal stiffness axes correspond then to the axes of the spacecraft frame.

It is clear that potential function, U, is minimized when the corresponding frame vectors are aligned.

Control torque The torque, $\boldsymbol{\tau}_{\mathrm{el}}^{\mathrm{scf}}$, corresponding to potential function (16) can be found by using a virtual work argument. Let $(\mathbf{A}_{\mathrm{sc}}^{\mathrm{eci}} + \mathbf{A}_{\mathrm{sc}}^{\mathrm{eci}} \delta\tilde{\boldsymbol{\theta}})$ be a virtual perturbation of the satellites attitude. The cross-product matrix $\delta\tilde{\boldsymbol{\theta}}$ is an arbitrary, infinitesimal rotation in spacecraft coordinates. The virtual work done by the displacement of the actual frame is

$$\delta W = -(\boldsymbol{\tau}_{\mathrm{el}}^{\mathrm{scf}})^t \delta\boldsymbol{\theta} = -\frac{1}{2}\mathrm{tr}((\tilde{\boldsymbol{\tau}}_{\mathrm{el}}^{\mathrm{scf}})^t \delta\tilde{\boldsymbol{\theta}}) \tag{19}$$

The virtual work has to be equal to the change in the energy function due to the displacement $\delta W = \delta U$ The torque, $\boldsymbol{\tau}_{\mathrm{el}}^{\mathrm{scf}}$ can be computed by computing the change in the potential function, δU, and equating that change with the virtual work, δW.

The change in the potential function due to the perturbation, $\delta\boldsymbol{\theta}$, of the attitude of the satellite is

$$\delta W = \delta U = U(\mathbf{A}_{\mathrm{sc}}^{\mathrm{eci}} + \mathbf{A}_{\mathrm{sc}}^{\mathrm{eci}} \delta\tilde{\boldsymbol{\theta}}) - U(\mathbf{A}_{\mathrm{sc}}^{\mathrm{eci}}) \tag{20}$$

where the dependence of U on the spacecraft attitude is shown explicitly. Using definition (16) of the potential function, obtain

$$\begin{aligned} \delta W &= \mathrm{tr}(\mathbf{P}) - \mathrm{tr}(\mathbf{P}(\mathbf{A}_{\mathrm{sc}}^{\mathrm{eci}} + \mathbf{A}_{\mathrm{sc}}^{\mathrm{eci}} \delta\tilde{\boldsymbol{\theta}})^t \mathbf{A}_{\mathrm{d}}^{\mathrm{eci}}) \\ &\quad - \mathrm{tr}(\mathbf{P}) + \mathrm{tr}(\mathbf{P}(\mathbf{A}_{\mathrm{sc}}^{\mathrm{eci}})^t \mathbf{A}_{\mathrm{d}}^{\mathrm{eci}}) \qquad (21) \\ &= -\mathrm{tr}(\mathbf{P}(\mathbf{A}_{\mathrm{sc}}^{\mathrm{eci}} \delta\tilde{\boldsymbol{\theta}})^t \mathbf{A}_{\mathrm{d}}^{\mathrm{eci}}) \qquad (22) \end{aligned}$$

where was used that in general $\mathrm{tr}(\mathbf{A}+\mathbf{B}) = \mathrm{tr}(\mathbf{A}) + \mathrm{tr}(\mathbf{B})$. For any skew-symmetric matrix it is true that $(\tilde{\mathbf{a}})^t = -\tilde{\mathbf{a}}$. Therefore the energy change can be written as

$$\delta W = \mathrm{tr}((\mathbf{A}_{\mathrm{sc}}^{\mathrm{eci}})^t \mathbf{A}_{\mathrm{d}}^{\mathrm{eci}} \mathbf{P} \delta\tilde{\boldsymbol{\theta}}) \tag{23}$$

because in general $\mathrm{tr}(\mathbf{AB}) = \mathrm{tr}(\mathbf{BA})$.

Any matrix $\mathbf{A}$ can be written as the sum of a symmetric and a skew-symmetric matrix: $\mathbf{A} = \mathrm{sym}(\mathbf{A}) + \mathrm{as}(\mathbf{A})$. The symmetric part is computed as $\mathrm{sym}(\mathbf{A}) = \frac{1}{2}(\mathbf{A} + \mathbf{A}^t)$ while the skew-symmetric part is given by $\mathrm{as}(\mathbf{A}) = \frac{1}{2}(\mathbf{A} - \mathbf{A}^t)$. This can be utilized to further simplify (23)

$$\delta W = \mathrm{tr}(\mathrm{sym}((\mathbf{A}_{\mathrm{sc}}^{\mathrm{eci}})^t \mathbf{A}_{\mathrm{d}}^{\mathrm{eci}} \mathbf{P}) \delta\tilde{\boldsymbol{\theta}} + \mathrm{as}((\mathbf{A}_{\mathrm{sc}}^{\mathrm{eci}})^t \mathbf{A}_{\mathrm{d}}^{\mathrm{eci}} \mathbf{P}) \delta\tilde{\boldsymbol{\theta}}) \quad (24)$$

For any symmetric matrix $\mathbf{A}$ and arbitrary vector $\mathbf{x}$, it is true that $\mathrm{tr}(\mathbf{A}\tilde{\mathbf{x}}) = 0$. Hence

$$\delta W = \mathrm{tr}((\mathrm{as}(\mathbf{P}(\mathbf{A}_{\mathrm{d}}^{\mathrm{eci}})^t \mathbf{A}_{\mathrm{sc}}^{\mathrm{eci}}))^t \delta\tilde{\boldsymbol{\theta}}) \quad (25)$$

From (19) and (25) we have that

$$-\frac{1}{2}\mathrm{tr}((\tilde{\boldsymbol{\tau}}_{\mathrm{el}}^{\mathrm{scf}})^t \delta\tilde{\boldsymbol{\theta}}) = \mathrm{tr}((\mathrm{as}(\mathbf{P}(\mathbf{A}_{\mathrm{d}}^{\mathrm{eci}})^t \mathbf{A}_{\mathrm{sc}}^{\mathrm{eci}}))^t \delta\tilde{\boldsymbol{\theta}}) \quad (26)$$

Because $\delta\boldsymbol{\theta}$ is arbitrary, the torque is given by

$$\tilde{\boldsymbol{\tau}}_{\mathrm{el}}^{\mathrm{scf}} = -2\mathrm{as}(\mathbf{P}(\mathbf{A}_{\mathrm{d}}^{\mathrm{eci}})^t \mathbf{A}_{\mathrm{sc}}^{\mathrm{eci}}) \quad (27)$$

This is the sought elastic control term. Carrying out the multiplication and operations yields

$$\boldsymbol{\tau}_{\mathrm{el}}^{\mathrm{scf}} = \begin{bmatrix} \pi_2(\mathbf{e}_{2,\mathrm{d}}^{\mathrm{eci}})^t \mathbf{e}_{3,\mathrm{sc}}^{\mathrm{eci}} - \pi_3(\mathbf{e}_{3,\mathrm{d}}^{\mathrm{eci}})^t \mathbf{e}_{2,\mathrm{sc}}^{\mathrm{eci}} \\ \pi_3(\mathbf{e}_{3,\mathrm{d}}^{\mathrm{eci}})^t \mathbf{e}_{1,\mathrm{sc}}^{\mathrm{eci}} - \pi_1(\mathbf{e}_{1,\mathrm{d}}^{\mathrm{eci}})^t \mathbf{e}_{3,\mathrm{sc}}^{\mathrm{eci}} \\ \pi_1(\mathbf{e}_{1,\mathrm{d}}^{\mathrm{eci}})^t \mathbf{e}_{2,\mathrm{sc}}^{\mathrm{eci}} - \pi_2(\mathbf{e}_{2,\mathrm{d}}^{\mathrm{eci}})^t \mathbf{e}_{1,\mathrm{sc}}^{\mathrm{eci}} \end{bmatrix} \quad (28)$$

The elastic term is easily computed given the frame vectors of the desired and actual frame.

Stiffness Matrix For small attitude errors the stiffness about one axis is the sum of the of the co-stiffnesses of the other two axes. This intuitive interpretation will be derived in this section.

For small attitude errors the attitude of the satellite can be expressed as $\mathbf{A}_{\mathrm{sc}}^{\mathrm{eci}} = \mathbf{A}_{\mathrm{d}}^{\mathrm{eci}} + \mathbf{A}_{\mathrm{d}}^{\mathrm{eci}} \delta\tilde{\boldsymbol{\theta}}$. From (27) it follows that the elastic term is

$$\tilde{\boldsymbol{\tau}}_{\mathrm{el}}^{\mathrm{scf}} = -2\mathrm{as}(\mathbf{P}(\mathbf{A}_{\mathrm{d}}^{\mathrm{eci}})^t(\mathbf{A}_{\mathrm{d}}^{\mathrm{eci}} + \mathbf{A}_{\mathrm{d}}^{\mathrm{eci}} \delta\tilde{\boldsymbol{\theta}}) \quad (29)$$

$$= -2\mathrm{as}(\mathbf{P}\delta\tilde{\boldsymbol{\theta}}) = -(\mathbf{P}\delta\tilde{\boldsymbol{\theta}} + \delta\tilde{\boldsymbol{\theta}}\mathbf{P}^t) \quad (30)$$

In general it is true that $\tilde{\mathbf{v}} = \mathbf{A}\tilde{\boldsymbol{\omega}} + \tilde{\boldsymbol{\omega}}\mathbf{A}^t$ iff $\mathbf{v} = (\mathrm{tr}(\mathbf{A})\mathbf{I}_3 - \mathbf{A}^t)\boldsymbol{\omega}$. Therefore

$$\boldsymbol{\tau}_{\mathrm{el}}^{\mathrm{scf}} = -\mathbf{K}\delta\boldsymbol{\theta} \quad (31)$$

where the stiffness matrix $\mathbf{K}$ is defined as

$$\mathbf{K} = \mathrm{tr}(\mathbf{P})\mathbf{I}_3 + \mathbf{P}^t = \mathrm{diag}(\pi_2 + \pi_3, \pi_1 + \pi_3, \pi_1 + \pi_2) \quad (32)$$

The stiffness about one axis is the sum of the co-stiffnesses of the other two axes. The selection of the stiffness matrix $\mathbf{K}$ is intuitive. Although the elastic term is nonlinear, for small attitude errors the $\mathbf{K}$ matrix has the same interpretation as the proportional gain of a linear controller. Once $\mathbf{K}$ is selected, the co-stiffness matrix is easily computed from

$$\mathbf{P} = \frac{1}{2}\mathrm{tr}(\mathbf{K})\mathbf{I}_3 - \mathbf{K}^t \quad (33)$$

4.2 Viscous Term

The viscous term is a damping term that provides stability. Let $\mathbf{B}$ be a diagonal[†], positive definite matrix of user selectable damping coefficients

$$\mathbf{B} = \mathrm{diag}(b_1, b_2, b_3) \quad (34)$$

The viscous term is the product of the damping matrix and the difference between the current and desired body rates in spacecraft coordinates

$$\boldsymbol{\tau}_{\mathrm{visc}}^{\mathrm{scf}} = \mathbf{B}(\boldsymbol{\omega}_{\mathrm{d}}^{\mathrm{scf}} - \boldsymbol{\omega}_{\mathrm{sc}}^{\mathrm{scf}}) \quad (35)$$

where $\boldsymbol{\omega}_{\mathrm{sc}}^{\mathrm{scf}}$ is the angular velocity of the satellite.

4.3 Model-Based Compensation Term

The model-based compensation term is based on the inverse model of the attitude dynamics of the satellite. This term would give the satellite the desired angular acceleration $\dot{\boldsymbol{\omega}}_{\mathrm{d}}^{\mathrm{scf}}$ in the absence of modeling and sensing errors.

The UASat can be modeled as a gyrostat[‡]. The attitude dynamics are given by[6, 4]

$$\dot{\boldsymbol{\omega}}_{\mathrm{sc}}^{\mathrm{scf}} = (\mathbf{I}_{\mathrm{sc}})^{-1}\left(\boldsymbol{\tau}_{\mathrm{ext}}^{\mathrm{scf}} + \boldsymbol{\tau}_{\mathrm{sc}}^{\mathrm{scf}} - \tilde{\boldsymbol{\omega}}_{\mathrm{sc}}^{\mathrm{scf}}\mathbf{h}^{\mathrm{scf}}\right) \quad (36)$$

$$\mathbf{h}^{\mathrm{scf}} = \mathbf{I}_{\mathrm{sc}}\boldsymbol{\omega}_{\mathrm{sc}}^{\mathrm{scf}} + \mathbf{E}_{\mathrm{rw}}\mathbf{I}_{\mathrm{rw}}(\boldsymbol{\omega}_{\mathrm{rw}} + (\mathbf{E}_{\mathrm{rw}})^t\boldsymbol{\omega}_{\mathrm{sc}}^{\mathrm{scf}}) \quad (37)$$

where $\mathbf{I}_{\mathrm{sc}}$ is the inertia matrix of the satellite with the reaction wheels unlocked, $\boldsymbol{\tau}_{\mathrm{ext}}^{\mathrm{scf}}$ are the external torques acting on the satellite, $\boldsymbol{\tau}_{\mathrm{sc}}^{\mathrm{scf}}$ are the internal torques acting on the satellite, $\mathbf{h}^{\mathrm{scf}}$ is the total angular momentum of the satellite, $\mathbf{E}_{\mathrm{rw}}$ is the reaction wheel configuration matrix, $\mathbf{I}_{\mathrm{rw}}$ is the diagonal matrix of reaction wheel inertias and $\boldsymbol{\omega}_{\mathrm{rw}}$ are the reaction wheel speeds. The matrix $\mathbf{E}_{\mathrm{rw}}$ depends on

[†]Any positive definite matrix can be used. However in this paper we choose $\mathbf{B}$ diagonal such that the principal axes correspond to the axes of the spacecraft frame.

[‡]A gyrostat is a mechanical system that consists of a rigid body $\mathcal{R}$ and one or more symmetrical rotors $\mathcal{W}_i$ whose axes are fixed in $\mathcal{R}$ and which are allowed to rotate with respect to $\mathcal{R}$ about their axes of symmetry.

the configuration of the reaction wheels and will be given in Sec. 4.4.

Assuming that the external torques are negligible, $\boldsymbol{\tau}_{\text{ext}}^{\text{scf}} \approx 0$, it follows from (36) that the actual angular acceleration matches the desired acceleration if the model-based compensation term is chosen as

$$\boldsymbol{\tau}_{\text{mdl}}^{\text{scf}} = \mathbf{I}_{\text{sc}}\dot{\boldsymbol{\omega}}_{\text{d}}^{\text{scf}} + \tilde{\boldsymbol{\omega}}_{\text{sc}}^{\text{scf}}\mathbf{h}^{\text{scf}} \tag{38}$$

4.4 Pseudo-Inverse

The sum of the elastic, viscous and model-based terms is an internal torque in spacecraft coordinates

$$\boldsymbol{\tau}_{\text{sc}}^{\text{scf}} = \boldsymbol{\tau}_{\text{visc}}^{\text{scf}} + \boldsymbol{\tau}_{\text{el}}^{\text{scf}} + \boldsymbol{\tau}_{\text{mdl}}^{\text{scf}} \tag{39}$$

The pseudo-inverse of the reaction wheel configuration matrix can be used to compute the reaction wheel torques that will produce this internal torque.

Let the reaction wheel configuration matrix, $\mathbf{E}_{\text{rw}}$, be the matrix with as columns the unit vectors in the direction of the spin axes of the reaction wheels

$$\mathbf{E}_{\text{rw}} = \begin{bmatrix} \mathbf{e}_{1,\text{rw}}^{\text{scf}} & \mathbf{e}_{2,\text{rw}}^{\text{scf}} & \mathbf{e}_{3,\text{rw}}^{\text{scf}} & \mathbf{e}_{4,\text{rw}}^{\text{scf}} \end{bmatrix} \tag{40}$$

where $\mathbf{e}_{\text{i,rw}}^{\text{scf}}$ is the unit vector in the direction of the spin axis of the i^{th} reaction wheel. The internal torque, $\boldsymbol{\tau}_{\text{sc}}^{\text{scf}}$, acting on the satellite structure due to the reaction wheel torques,$\boldsymbol{\tau}_{\text{rw}}$, is

$$\boldsymbol{\tau}_{\text{sc}}^{\text{scf}} = -\mathbf{E}_{\text{rw}}\boldsymbol{\tau}_{\text{rw}} \tag{41}$$

The reaction wheel configuration matrix, $\mathbf{E}_{\text{rw}}$, cannot be inverted as it is a 3×4 matrix. However, the pseudo-inverse can be used to find the reaction wheel torques, $\boldsymbol{\tau}_{\text{sc}}^{\text{rwf}}$, that produce the torque, $\boldsymbol{\tau}_{\text{sc}}^{\text{scf}}$, on the spacecraft structure

$$\boldsymbol{\tau}_{\text{sc}}^{\text{rwf}} = -(\mathbf{E}_{\text{rw}})^{\dagger}\boldsymbol{\tau}_{\text{sc}}^{\text{scf}} \tag{42}$$

where $(\mathbf{E}_{\text{rw}})^{\dagger}$ is the pseudo-inverse of $\mathbf{E}_{\text{rw}}$.

The reaction wheel configuration matrix $\mathbf{E}_{\text{rw}}$ depends on the actual configuration of the reaction wheels. The UASat design employs a pyramid-like configuration of the reaction wheels as shown in Fig. 4. The reaction wheel configuration matrix for this configuration is

$$\mathbf{E}_{\text{rw}} = \begin{bmatrix} 0 & 0 & 0.8165 & -0.8165 \\ 0 & -0.9428 & 0.4714 & 0.4714 \\ -1 & 0.3333 & 0.3333 & 0.3333 \end{bmatrix} \tag{43}$$

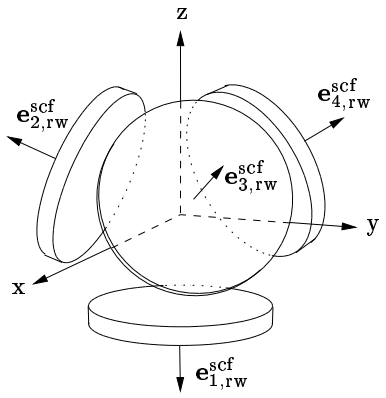

Figure 4: Geometry of the reaction wheels

and the pseudo-inverse is given by

$$(\mathbf{E}_{\text{rw}})^{\dagger} = \begin{bmatrix} 0 & 0 & -0.7500 \\ 0.0000 & -0.7071 & 0.2500 \\ 0.6124 & 0.3536 & 0.2500 \\ -0.6124 & 0.3536 & 0.2500 \end{bmatrix} \tag{44}$$

The value computed for $\boldsymbol{\tau}_{\text{sc}}^{\text{rwf}}$ in (42) is not unique. Torque vectors from the nullspace of $\mathbf{E}_{\text{rw}}$ can be added without changing the internal torque, $\boldsymbol{\tau}_{\text{sc}}^{\text{scf}}$, acting on the satellite structure. In fact, this is utilized in the next section to keep the reaction wheel speeds close to a desired speed.

4.5 Wheel Speed Management

It is desirable to keep the reaction wheel speeds above a certain level such that the bearings operate in the hydro-dynamic lubrication regime and zero-crossings are avoided. On the other hand, the reaction wheel speed should be kept low to decrease the power consumption. The wheel speed management term will try to keep the actual wheel speeds close to a specified desired speed $\boldsymbol{\omega}_{\text{rw,d}}$.

The speed of the reaction wheels can be controlled to a certain degree by adding a torque, $\boldsymbol{\tau}_{\text{wsm}}$, to the controller torque, $\boldsymbol{\tau}_{\text{sc}}^{\text{rwf}}$

$$\boldsymbol{\tau}_{\text{rw}} = \boldsymbol{\tau}_{\text{sc}}^{\text{rwf}} + \boldsymbol{\tau}_{\text{wsm}} \tag{45}$$

However, the wheel speed management torque, $\boldsymbol{\tau}_{\text{wsm}}$ cannot be chosen arbitrarily as it would produce a torque on the satellite structure. Therefore the wheel speed management torque is restricted to the null-space $\mathcal{N}(\mathbf{E}_{\text{rw}})$ of the reaction wheel configuration matrix. In that case, $\boldsymbol{\tau}_{\text{wsm}}$ will not contribute to the torque acting on the satellite structure because

$$\boldsymbol{\tau}_{\text{sc}}^{\text{scf}} = -\mathbf{E}_{\text{rw}}\boldsymbol{\tau}_{\text{sc}}^{\text{rwf}} - \mathbf{E}_{\text{rw}}\boldsymbol{\tau}_{\text{wsm}} = -\mathbf{E}_{\text{rw}}\boldsymbol{\tau}_{\text{sc}}^{\text{rwf}} \tag{46}$$

where the last equality follows from the fact that $\boldsymbol{\tau}_{\rm wsm} \in \mathcal{N}(\mathbf{E}_{\rm rw}) \Leftrightarrow \mathbf{E}_{\rm rw}\boldsymbol{\tau}_{\rm wsm} = \mathbf{0}$.

The reaction wheels are configured so that torque in any direction can be exerted on the spacecraft structure. That means that the spin axis unit vectors of any subset of three reaction wheels span the three dimensional space. Therefore matrix $\mathbf{E}_{\rm rw}$ has the maximum rank of 3 and the null-space has dimension one. Let $\mathbf{e}_{\mathcal{N}}$ by the unit vector that spans the null-space. The wheel speed management torque, $\boldsymbol{\tau}_{\rm wsm}$, is a scalar multiple, α, of this vector

$$\boldsymbol{\tau}_{\rm wsm} = \alpha \mathbf{e}_{\mathcal{N}} \tag{47}$$

The reaction wheel configuration matrix is given in (43). The unit vector spanning the null-space of $\mathbf{E}_{\rm rw}$ is given by $\mathbf{e}_{\mathcal{N}} = \begin{bmatrix} 0.5 & 0.5 & 0.5 & 0.5 \end{bmatrix}^t$

Define as error function, $V_{\rm rw}$, the sum of the squares of the deviations of the reaction wheel speeds from their desired values

$$V_{\rm rw} = \frac{1}{2}(\Delta\boldsymbol{\omega}_{\rm rw})^t \Delta\boldsymbol{\omega}_{\rm rw} \tag{48}$$

where $\Delta\boldsymbol{\omega}_{\rm rw} = \boldsymbol{\omega}_{\rm rw,d} - \boldsymbol{\omega}_{\rm rw}$. The scalar, α, will be selected such that this error function decreases. Assuming that the desired reaction wheel speeds are constant, the time derivative of the error function is

$$\frac{d}{dt}V_{\rm rw} = -(\Delta\boldsymbol{\omega}_{\rm rw})^t \frac{d}{dt}\boldsymbol{\omega}_{\rm rw} \tag{49}$$

For each wheel the change in speed is the motor torque divided by the moment of inertia of the wheel about its spin axis minus the acceleration of the satellite structure in the direction of the spin axis[4]

$$\frac{d}{dt}V_{\rm rw} = -(\Delta\boldsymbol{\omega}_{\rm rw})^t(\mathbf{I}_{\rm rw}^{-1}\boldsymbol{\tau}_{\rm rw} - (\mathbf{E}_{\rm rw})^t\dot{\boldsymbol{\omega}}_{\rm sc}^{\rm scf}) \tag{50}$$

where $\mathbf{I}_{\rm rw}$ is the diagonal matrix with the inertias of the reaction wheels about their spin axes on its diagonal. Substitution of (45) and (47) yields

$$\frac{d}{dt}V_{\rm rw} = -(\Delta\boldsymbol{\omega}_{\rm rw})^t(\mathbf{I}_{\rm rw}^{-1}\boldsymbol{\tau}_{\rm sc}^{\rm rwf} - (\mathbf{E}_{\rm rw})^t\dot{\boldsymbol{\omega}}_{\rm sc}^{\rm scf}) - (\Delta\boldsymbol{\omega}_{\rm rw})^t\mathbf{I}_{\rm rw}^{-1}\mathbf{e}_{\mathcal{N}}\alpha \tag{51}$$

The first term does not contain α and cannot be influenced. However, the second term does contain α and should be made negative. The second term is negative when α is chosen as

$$\alpha = k_{\rm wsm}(\Delta\boldsymbol{\omega}_{\rm rw})^t\mathbf{I}_{\rm rw}^{-1}\mathbf{e}_{\mathcal{N}} \tag{52}$$

where $k_{\rm wsm}$ is a positive, user selectable, proportionality gain. The wheel speed management torque follows from (47)

$$\boldsymbol{\tau}_{\rm wsm} = k_{\rm wsm}(\Delta\boldsymbol{\omega}_{\rm rw})^t(\mathbf{I}_{\rm rw}^{-1}\mathbf{e}_{\mathcal{N}})\mathbf{e}_{\mathcal{N}} \tag{53}$$

As mentioned previously, the first term of the right hand side of (51) cannot be influenced and the second term cannot be made arbitrarily negative. Therefore, as one would expect, the error, $V_{\rm rw}$, is not guaranteed to always decrease.

If one of the reaction wheels fails a column of $\mathbf{E}_{\rm rw}$ is effectively removed resulting in a nonsingular 3×3 matrix. The nullspace is reduced to the origin and wheel speed management can no longer be used.

5 Simulations

The control law and the kinematics have been simulated using Matlab. The results presented in this section are for tracking of a ground station located in Tucson ($\lambda_{\rm N} = 32.19581°$, $\lambda_{\rm W} = -110.89171°$).

5.1 Controller Parameters

The parameters of the elastic and viscous feedback term are the damping matrix, $\mathbf{B}$, and the stiffness matrix, $\mathbf{K}$. The damping matrix is chosen as

$$\mathbf{B} = \text{diag}(1.17, 1.17, 1.17) \text{ Nms/rad} \tag{54}$$

and the stiffness matrix is chosen as

$$\mathbf{K} = \text{diag}(0.32, 0.32, 0.32) \text{ Nm/rad} \tag{55}$$

In order to compute the model-based feed-forward term, estimates of the satellite inertia, reaction wheel inertias and the reaction wheel configuration matrix are required. The estimated reaction wheel configuration matrix is given in (43). The estimated moments of inertia of the reaction wheels are $I_{\rm rw,1} = I_{\rm rw,2} = I_{\rm rw,3} = I_{\rm rw,4} = 0.6452 \cdot 10^{-3}$ kg m^2. The estimated inertia of the satellite is

$$\mathbf{I}_{\rm sc} = \text{diag}(2.66, 2.66, 2.263) \text{ kg m}^2 \tag{56}$$

The desired reaction wheel speed is specified as $\boldsymbol{\omega}_{\rm rw,d} = 750$ rpm and the wheel speed management gain is chosen as $k_{\rm wsm} = 0.03$ s^{-1}. A sample time of $t_{\rm s} = 0.25$ s was used for the controller.

5.2 Simulation Model

The simulation model includes attitude dynamics, orbital kinematics, aerodynamic drag, and reaction

wheel models. Although an attitude estimation algorithm based on Kalman filtering is (partially) implemented, a perfect attitude estimate is used so that the pointing error is only due to control errors.

Initial studies showed that the aerodynamic drag torque is on the order of 5×10^{-5} Nm, an order of magnitude larger than solar pressure and gravity gradient disturbance torques. The residual magnetic dipole moment cannot be determined yet but is assumed to be much smaller than the aerodynamic drag torque. Therefore only the aerodynamic drag torque is included in the environmental model.

To make the simulations more realistic, modeling errors are introduced in two ways. First, the actual parameters used to simulate the equations of motion are different than the estimated parameters used in the model-based term of the control law as given in Sec. 5.1. Second, the reaction wheel models include friction and limited torque capabilities. The actual inertia of the satellite is assumed to be

$$\mathbf{I}_{sc} = \begin{bmatrix} 2.7388 & -0.0031 & -0.0269 \\ -0.0031 & 2.7924 & 0.0136 \\ -0.0269 & 0.0136 & 2.1741 \end{bmatrix} \text{kg m}^2 \quad (57)$$

which corresponds to a maximum of 4° deviation of the actual from the estimated principal axes of inertia and a maximum error of 5% in the moments of inertia about those axes. The actual reaction wheel configuration matrix is assumed to be

$$\mathbf{E}_{rw} = \begin{bmatrix} 0.056 & 0.033 & 0.817 & -0.817 \\ 0.038 & -0.945 & 0.453 & 0.453 \\ -0.998 & 0.324 & 0.358 & 0.358 \end{bmatrix} \quad (58)$$

which corresponds to a misalignment of the spin-axes of 3.85°, 1.97°, 1.75°, and 1.75°, with respect to the estimated spin-axes.

The reaction wheel models include viscous and coloumb friction, constant, quiescent electronic losses, motor efficiency and limited torque capability. The actual parameters of the reaction wheels are given in Tab. 4. The actual moments of inertia of the reaction wheels about their spin axis differ by a maximum of 4% from the estimated values used in the control law.

5.3 Simulation Results

Figure 5 shows the pointing error which is defined as the angle between the telescope axis and the z-axis of the desired frame. Rotations around the telescope axis are not considered as they are not important.

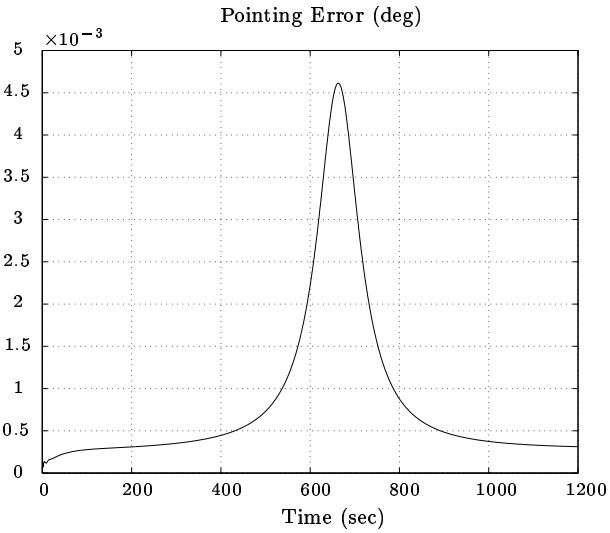

Figure 5: Pointing error as a function of time.

The maximum error is smaller than $5 \cdot 10^{-3}$ degree and occurs when the satellite is right above Tucson at 662s. The maximum error is well below the required 1° pointing accuracy. Simulation runs with different sampling intervals and without the model based compensation showed that the control error is dominated by the error due to sampling. However, the overall pointing error will likely be dominated by the sensing error and be much larger.

Figure 6 shows the reaction wheel torques during the maneuver. The maximum commanded torque is smaller than 10^{-3} Nm which is well below the maximum torque capability of $7.4 \cdot 10^{-3}$ Nm. There is no saturation of the reaction wheel torques.

Figure 7 shows the reaction wheel speeds as a function of time. Initially at $t = 0$, the wheel speeds are higher than the desired speeds of 750 rpm. The wheel speed management term brings the speed back to desired speed. At $t = 662s$ the satellite is above Tucson and the speed of reaction wheel 4 reaches a minimum. However, due to the wheel speed bias the speed of reaction wheel 4 does not cross zero. The speeds of the reaction wheels stay well below the maximum speed of 8000 rpm.

Figure 8 shows the total power drawn by the reaction wheels as a function of time. Initially, all reaction wheels are slowed resulting in a reduced power consumption. Around $t = 662s$ the power consumption varies due to a variation in the speed of the wheels. However, overall the power consumption is dominated by the constant electronic losses ($4 \cdot 1.7708 = 7.08$W).

		RW1	RW2	RW3	RW4	
Rotor inertia	$I_{\mathrm{rw},}$	0.6387	0.6710	0.6194	0.6581	10^{-3} kg m^2
Max. speed		8,000	8,000	8,000	8,000	rpm
Max. torque	$\tau_{\max}$	7.4	7.4	7.4	7.4	10^{-3} Nm
Electr. losses	P_{eca}	1.7708	1.7708	1.7708	1.7708	W
Viscous friction	r_{drag}	0.3305	0.3827	0.3653	0.3131	10^{-6} Nms/rad
Coulomb friction	τ_{cl}	0.3045	0.2896	0.2747	0.3195	10^{-3} Nm
Motor efficiency	η	0.9	0.9	0.9	0.9	
Torque gain		0.95	1.08	0.91	1.09	

Table 4: Actual parameters of reaction wheel models.

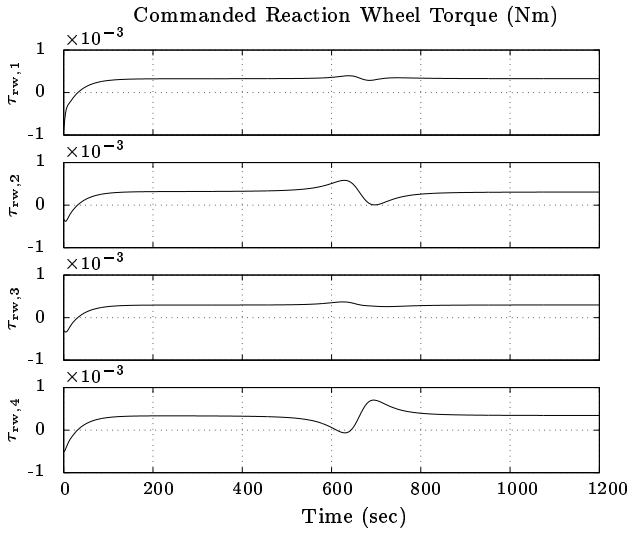

Figure 6: Commanded reaction wheel torques as a function of time.

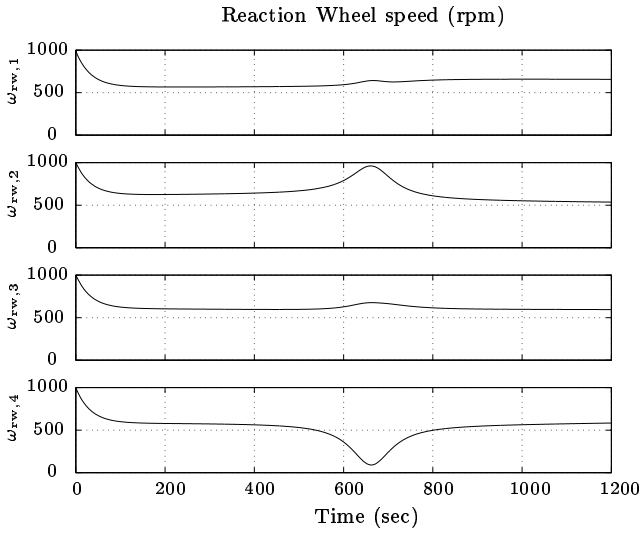

Figure 7: Reaction wheel speeds as a function of time.

6 Summary and Discussion

The UASat is a small satellite being designed by students from The University of Arizona to be launched from the Hitchhiker Ejection System. One of its missions is to receive laser communication signals from a ground station. In order to receive these signals, the telescope must be pointing at the ground station while passing over. Kinematics equations were presented for this motion.

A geometric nonlinear control law is used to track the desired motion specified by the kinematics. Feedback is provided by an elastic and a viscous term. The elastic term implements a spatial spring-like behavior between the desired and actual frame. The viscous term is a damping term that depends on the difference between the actual and desired angular velocity. Model-based compensation is provided by a feed-forward term based on the inverse of the attitude dynamics. The wheel speed management term lets the reaction wheels operate around a desired speed such that zero-crossings of the wheel speeds are avoided during the maneuver. The wheel speed bias also ensures that the wheel bearings operate in the hydro-dynamic lubrication regime.

The elastic term is parameterized by a co-stiffness matrix $\mathbf{P}$. It was shown that for small attitude errors the stiffnesses about each axis of the spacecraft frame is the sum of the co-stiffnesses about the other two axes. The viscous term is parameterized by a damping matrix $\mathbf{B}$. Similarly, for small attitude errors the damping factors correspond to viscous damping coefficients about each axis of the spacecraft frame. The intuitive, geometric interpretation simplifies the selection of the control parameters.

A simulation was performed for tracking a ground

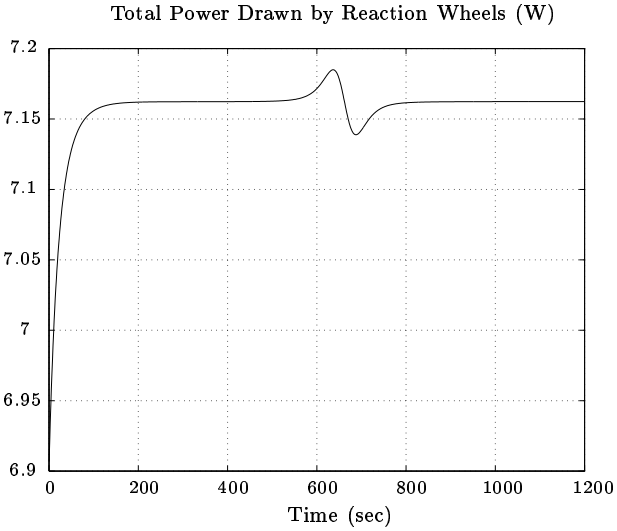

Figure 8: Total power draw by reaction wheels as a function of time.

station located in Tucson. This simulation showed that the commanded reaction wheel torques are smaller than the maximum torques. Also, the speeds of the reaction wheels stayed well under their maximum values. This indicates that the ground tracking maneuver can be performed successfully with available reaction wheels.

For large attitude errors the commanded reaction wheel torques will exceed their maximum torque capability. However, saturation of the reaction wheel torques is not accounted for in the controller. To avoid large attitude errors and saturation, a desired attitude profiler should be used for switching modes and switching targets within modes.

In this paper it was assumed that an accurate attitude estimate was available. With the current design, the attitude estimation error will dominate the overall pointing error. A Kalman filter has been designed and partially implemented. Implementation, testing and analysis of the estimation system is ongoing and will be reported later.

7 Acknowledgments

Brian Shucker was partially supported by a NASA Space Grant Internship and an honors grant of The University of Arizona. Barry Goeree was partially supported by a Cariñoso Scholarship. The authors gratefully acknowledge this support. The authors like to thank the GNC-team for their support and help, especially Greg Chatel and David Faulkner who helped with the simulations and obtaining the model parameters. Furthermore, we like to thank Tupper Hyde and Dave Miller of Honeywell Space Systems and Doug Havenhill of SatCon Technology Corporation for their valuable comments on the original manuscript.

References

[1] Peter E. Crouch. Spacecraft attitude control and stabilization: Applications of geometric control theory to rigid body models. *IEEE Transactions on Automatic Control*, AC-29(4):321–331, April 1984.

[2] Thomas A.W. Dwyer III. Exact nonlinear control of large angle rotational maneuvers. *IEEE Transactions on Automatic Control*, AC-29(9):769–774, September 1984.

[3] Thomas A.W. Dwyer III and H. Sira-Ramirez. Variable structure control of spacecraft attitude maneuvers. *AIAA Journal of Guidance, Control and Dynamics*, 11:262–270, 1988.

[4] Barry B. Goeree and Greg Chatel. Attitude dynamics of the UASat. technote GNC-013, Student Satellite Project, University of Arizona, Tucson, AZ, April 1999. Available from http:// uasat.arizona.edu/ ssp/ documents/ technotes/.

[5] Barry B. Goeree and Brian Shucker. Kinematics of ground station tracking. technote GNC-0012, Student Satellite Project, University of Arizona, Tucson, AZ, April 1999. Available from http:// uasat.arizona.edu/ ssp/ documents/ technotes/.

[6] Peter C. Hughes. *Spacecraft Attitude Dynamics*. John Wiley & Sons, New York, 1986.

[7] M. Kayton and W.R. Fried. *Avionics Navigation Systems*. Wiley-Interscience, second edition, 1997.

[8] Daniel E. Koditschek. The application of total energy as a Lyapunov function for mechanical control systems. *Contemporary Mathematics*, 97:131–157, February 1989.

[9] Chris A. Lewicki and K.C. Hsieh. UASat: a student satellite project. In *Proceedings of the 12th AIAA/USU Conference on Small Satellites*. Utah State University, September 1998.

[10] George Meyer. Design and global analysis of spacecraft attitude control systems. NASA Technical Report TR R-361, Ames Research Center, Moffet Field, CA, 1971.

[11] Russell A. Paielli and Ralp E. Bach. Attitude control with realization of linear error dynamics. *AIAA Journal of Guidance, Control and Dynamics*, 16(1):182–189, 1993.

[12] R.D. Robinett and G.G. Parker. Spacecraft Euler parameter tracking of large angle maneuvers via sliding mode control. *AIAA Journal of Guidance, Control and Dynamics*, 19:702–703, 1996.

[13] M.D. Shuster. A survey of attitude representations. *J. of the Astronautical Sciences*, 41:439–517, 1993.

[14] Panagiotis Tsiotras. Stabilization and optimality results for the attitude control problem. *AIAA Journal of Guidance, Control and Dynamics*, 19(4):772–779, 1996.

[15] James R. Wertz. *Spacecraft Attitude Determination and Control*, chapter 18. Reidel, Dordrecht, The Netherlands, 1978.